Research Square

Preprints are preliminary reports that have not undergone peer review.
They should not be considered conclusive, used to inform clinical practice,
or referenced by the media as validated information.

Neurofeedback reveals cognitive states supporting waking human hippocampal ripples

Takufumi Yanagisawa

tyanagisawa@nsurg.med.osaka-u.ac.jp

The University of Osaka https://orcid.org/0000-0002-2057-0612

Takamitsu Iwata

Osaka University https://orcid.org/0000-0003-2533-0551

Yuji Ikegaya

The University of Tokyo https://orcid.org/0000-0003-2260-8191

Ryohei Fukuma

Osaka University https://orcid.org/0000-0002-3316-9561

Satoru Oshino

Department of Neurosurgery, Graduate School of Medicine, Osaka University https://orcid.org/0000-0002-4248-2322

Naoki Tani

Department of Neurosurgery, Graduate School of Medicine, Osaka University https://orcid.org/0000-0003-2169-135X

Hui Ming Khoo

Department of Neurosurgery, Graduate School of Medicine, Osaka University https://orcid.org/0000-0002-4039-0520

Yasushi Iimura

Juntendo University

Hiroharu Suzuki

Juntendo University

Takumi Mitsuhashi

Juntendo University https://orcid.org/0000-0001-8156-5385

Haruhiko Kishima

Osaka University https://orcid.org/0000-0002-9041-2337

Article

Keywords:

Posted Date: November 20th, 2026

DOI: https://doi.org/10.21203/rs.3.rs-11492575/v1

License: This work is licensed under a Creative Commons Attribution 4.0 International License.
Read Full License

Additional Declarations: There is **NO** Competing Interest.

Abstract

Hippocampal sharp-wave ripples contribute to memory processing during sleep and wakefulness, but how their occurrence varies with intentional changes in cognitive states remains unclear. Here, we examined hippocampal ripple occurrence during intentional state regulation across different cognitive conditions. Nine participants who underwent intracranial monitoring for epilepsy attempted to increase feedback derived from online hippocampal ripple detection during free thought, instructed relaxation (Calm) and mental calculation. Offline analyses revealed higher ripple rates during free-thought neurofeedback than during pre-block periods without feedback and higher rates during Calm than during free thought or calculation. Calm-related increases were consistent across participants and persisted under stringent ripple-selection criteria. Ripple rates covaried positively with cortical delta power, and delta-ripple relationships varied across cognitive conditions, whereas lower self-reported feedback monitoring was associated with higher ripple rates. These findings reveal that waking hippocampal ripple expression varies systematically with cognitive context and is modulated during intentional cognitive-state regulation.

Introduction

Human cognition depends on the reactivation of stored representations to retrieve past experiences and guide ongoing behavior. Hippocampal sharp-wave ripples—brief, high-frequency population events—are closely associated with the reactivation of memory representations and have been implicated in memory consolidation and retrieval[1–3]. Although ripples are most prominent during nonrapid-eye-movement sleep and quiet wakefulness, their strong dependence on the brain state suggests that their occurrence might also be influenced by deliberate shifts in cognitive states. Changes in thought, attention or arousal could therefore alter the physiological conditions under which ripples emerge. If humans can intentionally increase ripple occurrence by adopting particular cognitive states, this would provide a means to determine whether cognitive strategies can be used to recruit endogenous hippocampal activity associated with memory processing and to examine the functional consequences of such modulation. However, whether intentional cognitive-state regulation can reliably increase hippocampal ripple expression in humans and the cognitive states that are most favorable for ripple occurrence remain unknown.

Human intracranial studies increasingly indicate that hippocampal ripples are embedded within distributed hippocampal–cortical dynamics rather than confined to local hippocampal activity. During episodic retrieval, ripple activity in the medial temporal lobe and neocortex becomes temporally coupled, and this coupling is associated with the reinstatement of cortical representations of remembered information[4]. Hippocampal ripples can also precede content-specific reinstatement of higher-order cortical activity during spontaneous recollection, whereas more recent studies have linked ripple occurrence to dynamic changes in cortical representations during retrieval, planning and inference[5–7]. Collectively, these findings suggest that waking hippocampal ripples participate in large-scale neural dynamics, supporting the reinstatement and reorganization of memory-related representations.

Waking hippocampal ripples have also been linked to episodic recollection and to internally generated representations of past events and possible future experiences[5,8,9]. However, previous work has primarily examined the cognitive, behavioral, and physiological conditions under which ripples arise spontaneously, and whether ripple occurrence can be systematically influenced through intentional changes in cognitive states remains unclear. Wakeful cognition varies in the degree to which it is constrained by externally imposed goals and ongoing task demands versus generated more freely from internal representations. Theories of spontaneous thought describe cognition along a continuum from strongly goal-constrained processing to freely self-generated thought[10–12]. Consistent with this framework, hippocampal ripples occur more frequently during naturally occurring self-generated thought when cognition is less tightly coupled to external tasks[13]. Reduced external constraints may therefore constitute one cognitive context that favors waking ripple occurrence. However, because reduced task engagement can also coincide with changes in arousal, the contribution of cognitive constraints cannot be considered independent of the state of the brain.

Real-time neurofeedback offers an experimental approach to probe whether intentional changes in cognitive states are associated with changes in ongoing neural activity because participants can adopt different cognitive strategies while receiving feedback derived from that activity[14]. We therefore used real-time feedback based on hippocampal ripple detection to test whether participants could discover and adopt cognitive states associated with increased ripple occurrence. Importantly, this framework does not assume that ripple neurofeedback directly induces shifts between externally and internally oriented cognition. Instead, it enables characterization of the cognitive and neurophysiological conditions accompanying variations in ripple expression.

Here, we investigated whether humans can increase the occurrence of waking hippocampal ripples during intentional cognitive-state regulation supported by real-time intracranial neurofeedback. Participants attempted to increase the visual feedback signal derived from online hippocampal ripple detection while engaging in different instructed cognitive states. We first assessed whether ripple occurrence increased relative to that in brief pre-block periods without feedback and then compared the effects of different types of cognitive instructions. Based on evidence linking waking ripples to less externally constrained cognitive states and quiet wakefulness, we hypothesized that instructed calm relaxation would be associated with the greatest increase in ripple occurrence, potentially reflecting reduced task engagement and concomitant changes in arousal. Finally, we examined participants' subjective reports and concurrent cortical spectral activity to identify the cognitive and neurophysiological correlates of elevated ripple occurrence.

Results

Real-time visual neurofeedback was driven by the online detection of hippocampal ripples

We provided real-time hippocampal ripple neurofeedback to nine participants who underwent intracranial electroencephalogram (EEG) monitoring for clinical evaluation (Supplementary Fig. 1). Ripple events were detected online from a bipolar hippocampal channel using predefined frequency, amplitude and duration criteria (Methods). The detected events were translated into visual feedback by modulating the size of a circle displayed on a monitor (Fig. 1a). The locations of the hippocampal contacts used for online ripple detection are shown in Fig. 1b.

During each 10-min neurofeedback block, participants were instructed to make the feedback circle as large as possible. Except when a specific cognitive strategy was prescribed by the experimental condition, participants received no instructions about how to achieve this goal and were encouraged to explore different mental strategies to increase the feedback signal.

To characterize the events detected during neurofeedback, we analyzed the corresponding hippocampal local field potentials offline (Supplementary Figs. 2 and 3). Across all the detected hippocampal ripples, the mean peak frequency was 96.1 ± 10.8 Hz, and the mean duration was 67.2 ± 7.8 ms (mean ± s.d. across participants, n = 9). Event-triggered averaging revealed a stereotyped ripple-band oscillation around the detection onset, as well as a transient increase in the ripple-band power in the time–frequency representation (Fig. 1c and d; Supplementary Figs. 4 and 5). Inter-ripple intervals had a median duration of 2.31 s (Fig. 1e). Furthermore, the distribution of the cortical delta-band activity coincident with ripple occurrence provided an additional measure of the cortical state in which the detected ripples occurred (Fig. 1f; Supplementary Fig. 6).

Waking hippocampal ripple occurrence depended on the cognitive state during neurofeedback

The experiment involved Free, Calm and Calculation conditions for all nine participants, with Meditation also performed by six participants (Methods). These conditions were designed to span relatively unconstrained thought, calm relaxation, effortful mental arithmetic and internally directed attention states, respectively.

We first asked whether ripple occurrence differed from the no-neurofeedback baseline using exposure-adjusted Poisson mixed-effects models (Methods). In the primary ALL event set, the median ripple rate increased from 1.39 events min^{-1} at baseline to 3.23 events min^{-1} during free neurofeedback (rate ratio (RR) = 2.15, 95% CI 1.36–3.39, FDR-adjusted P = 0.0036; Fig. 2a). The ripple rates of seven of the nine participants increased, and the effect remained positive in all leave-one-participant-out analysis (RR range, 1.72–2.52).

The occurrence of ripples increased further under the Calm condition. The median ripple rate was 5.46 events min^{-1}, corresponding to a 2.91-fold increase relative to baseline (RR = 2.91, 95% CI 1.85–4.57, FDR-adjusted P = 5.22×10^{-4}). The ripple rates of eight of the nine participants increased in the Calm condition relative to baseline. Furthermore, significantly more ripples occurred under the Calm condition

than under the Free condition (Calm/Free RR = 1.49, 95% CI 1.30–1.71, FDR-adjusted P = 1.59×10^{-5}; Fig. 2a), with the same effect direction observed in seven of the nine participants. The Calm-versus-baseline effect was also stable in leave-one-participant-out analyses (RR range, 2.04–3.61).

The ripple occurrence rate was similarly elevated under the Meditation condition in the six participants who performed this condition. The ripple rate was greater under the Meditation condition than at baseline (RR = 3.16, 95% CI 1.75–5.68, FDR-adjusted P = 0.0029) and greater than that under the Free condition (Meditation/Free RR = 1.25, 95% CI 1.05–1.50, FDR-adjusted P = 0.0225). No statistically detectable difference was observed between the Meditation and Calm condition (Meditation/Calm RR = 0.94, 95% CI 0.79–1.10, FDR-adjusted P = 0.387). Because this comparison involved only six participants, we treated the Meditation findings as supportive rather than as a primary test of the condition differences.

In contrast, a distinct pattern was observed under the Calculation condition. The ripple rate under the Calculation condition did not differ from that at baseline (RR = 1.13, 95% CI 0.71–1.80, FDR-adjusted P = 0.589) and was lower than under the Free (Calculation/Free RR = 0.55, 95% CI 0.46–0.65, FDR-adjusted P = 4.76×10^{-6}) and Calm conditions (Calm/Calculation RR = 2.66, 95% CI 2.25–3.14, FDR-adjusted P = 6.59×10^{-9}). This condition specificity argues against a nonspecific increase in ripple occurrence during neurofeedback or sustained cognitive effort.

Exploratory analyses of individual ripple characteristics provided more limited evidence for condition-dependent changes (Supplementary Fig. 7). The participant-level median ripple duration was nominally longer under the Calm condition than under the Free condition (median paired difference [Calm − Free], 5.75 ms; paired Wilcoxon signed-rank test, P = 0.0156) and the Meditation condition (median paired difference [Calm − Meditation], 6.88 ms; P = 0.0313). However, neither difference remained significant after FDR correction across the six pairwise condition comparisons (both FDR-adjusted P = 0.0938; Fig. 2b).

The principal condition structure was preserved when analyses were restricted to the more stringently defined HC event set (Fig. 2c). The ripple rate under the Calm condition remained elevated relative to baseline (RR = 2.50, 95% CI 1.55–4.01, FDR-adjusted P = 0.00347) and to the Free condition (Calm/Free RR = 1.62, 95% CI 1.38–1.89, FDR-adjusted P = 1.97×10^{-5}), whereas the ripple rate under the Calculation condition remained lower than that under the Free condition (Calculation/Free RR = 0.55, 95% CI 0.45–0.68, FDR-adjusted P = 2.39×10^{-5}). The direction of the baseline-to-Free effect was preserved, but the effect was attenuated and did not survive FDR correction (RR = 1.66, 95% CI 1.03–2.69, FDR-adjusted P = 0.0536). Because HC events constitute a subset of the ALL event set, this analysis tests robustness to the stringency of the event definition rather than providing an independent replication.

The displayed feedback magnitude was numerically greater under the Calm condition than under the Calculation condition, although this comparison was not significant after Holm correction (mean

difference [Calculation − Calm] = − 1.02, 95% CI − 2.15 to 0.12, P = 0.072, Holm-adjusted P = 0.217; Fig. 2d).

Ripple rates increased during later portions of Calm condition blocks

We next examined the temporal evolution of ripple expression within neurofeedback blocks using 2-min bins. A Poisson mixed-effects model of Ripple counts with time, condition and their interaction, adjusted for valid recording time, showed a significant overall condition effect ($F(2,262) = 14.19$, $P = 1.41 \times 10^{-6}$), whereas neither the main effect of time ($F(1,262) = 1.02$, $P = 0.313$) nor the condition-by-time interaction was significant ($F(2,262) = 1.29$, $P = 0.277$; Fig. 2e). To further characterize whether ripple expression differed between earlier and later portions of the block without assuming a specific transition time, we performed an exploratory analysis in which each block was divided into early and later periods while systematically varying the boundary from 1 to 5 min. Under the Calm condition, the estimated later/early rate ratio was greater than 1 at every boundary: 2.02 (95% CI 1.36–3.00, P = 0.00085) for a 1-min cutoff, 1.64 (1.27–2.13, P = 0.00036) for a 2-min cutoff, 1.34 (1.09–1.64, P = 0.0064) for a 3-min cutoff, 1.16 (0.97–1.39, P = 0.109) for a 4-min cutoff and 1.24 (1.04–1.47, P = 0.018) for a 5-min cutoff. After correction across the five alternative cutoffs, the effects remained significant for the 1-, 2-, 3- and 5-min boundaries (FDR-adjusted P = 0.0021, 0.0018, 0.0106 and 0.0225, respectively; Fig. 2f; also see Supplementary Fig. 8).

The corresponding pattern was less consistent under the other conditions. Under the Free condition, the ripple rate was higher after the first minute (Later/Early rate ratio = 1.98, 95% CI 1.28–3.08, P = 0.0030, FDR-adjusted P = 0.015), whereas the effects observed when boundaries of 2 to 5 min were observed were smaller and not significant (rate ratios = 1.06–1.23, all FDR-adjusted $P \geq 0.212$). Under the Calculation condition, no significant later/early difference was detected at any of the examined boundaries (rate ratios = 1.00–1.27, all FDR-adjusted $P \geq 0.795$). Thus, whereas an initial first-minute difference was observed under the Free condition, broader and more persistent increases in ripple expression were observed during later portions of the Calm block.

Cortical–hippocampal coupling varied with the cognitive condition

We next asked whether the cognitive conditions associated with different ripple rates were accompanied by changes in cortical spectral activity or its moment-to-moment relationship with ripple expression. For each participant, spectral power was quantified across cortical electrodes in the delta (1–4 Hz), theta (4–8 Hz), alpha (8–13 Hz), beta (13–30 Hz), low-gamma (30–60 Hz), and high-gamma (70–150 Hz) bands (Fig. 3a).

Mean cortical spectral power showed condition-dependent differences in the theta and alpha bands. Significant condition effects were observed for theta power ($F(2,24) = 8.32$, $P = 0.0018$, FDR-adjusted $P = 0.0054$) and alpha power ($F(2,24) = 14.27$, $P = 8.26 \times 10^{-5}$, FDR-adjusted $P = 4.96 \times 10^{-4}$), whereas no

significant condition effects were observed for delta, beta, low-gamma or high-gamma power after FDR correction across the six frequency bands (Supplementary Fig. 9).

Despite these condition-dependent differences in theta and alpha power, moment-to-moment cortical activity covaried systematically with ripple occurrence. Across 260 valid 60-s windows from the nine participants, the ripple rate was positively associated with delta power (β = 1.55 events min − 1 per s.d., 95% CI 0.92–2.18, q = 1.41×10^{-5}), theta power (β = 1.47, 95% CI 0.79–2.14, q = 6.52×10^{-5}), alpha power (β = 1.54, 95% CI 0.82–2.26, q = 6.52×10^{-5}) and beta power (β = 1.01, 95% CI 0.37–1.65, q = 0.00335). The associations with low-gamma (β = −0.31, 95% CI − 1.01 to 0.39, q = 0.381) and high-gamma power (β = −0.66, 95% CI − 1.37 to 0.04, q = 0.077) did not survive FDR correction (Fig. 3b).

Critically, several cortical–ripple relationships depended on the cognitive condition. Significant band-power-by-condition interactions were observed for delta (likelihood-ratio $\chi^2(2) = 8.51$, P = 0.0142, q = 0.0284), low-gamma ($\chi^2(2) = 11.91$, P = 0.00259, q = 0.00777) and high-gamma power ($\chi^2(2) = 14.55$, P = 6.91×10^{-4}, q = 0.00415), but not for theta, alpha or beta power (Supplementary Fig. 10).

The delta–ripple relationship varied significantly across cognitive conditions (likelihood-ratio $\chi^2(2) = 8.51$, P = 0.0142, q = 0.0284; Fig. 3c). Under the Free condition, a 1-s.d. increase in delta power was associated with 1.55 additional ripples min − 1 (95% CI 0.28–2.81, P = 0.0167). The estimated delta–ripple slope was steeper under the Calm condition (estimated slope, 3.23 events min − 1 per s.d.); however, the Calm-by-delta contrast relative to Free did not reach nominal significance (interaction β = 1.68, 95% CI − 0.08 to 3.43, P = 0.0606). The corresponding interaction under the Calculation condition was also not significant (β = −0.91, 95% CI − 2.59 to 0.76, P = 0.283).

A complementary pattern emerged at high frequencies. The high-gamma–ripple relationship varied significantly across cognitive conditions (likelihood-ratio $\chi^2(2) = 14.55$, P = 6.91 × 10 − 4, q = 0.00415; Fig. 3d). Under the Free condition, high-gamma power was negatively associated with the ripple rate (β = −1.99 events min − 1 per s.d., 95% CI − 3.26 to − 0.73, P = 0.0021). This relationship was significantly altered under the Calculation condition (Calculation × high-gamma interaction: β = 3.37 events min − 1 per s.d., 95% CI 1.53–5.21, P = 3.80×10^{-4}), whereas the corresponding interaction under the Calm condition was not significant (β = 0.59, 95% CI − 1.31 to 2.49, P = 0.544).

Together, these results indicate that cognitive condition was associated with both differences in mean cortical spectral activity and condition-dependent relationships between ongoing cortical activity and hippocampal ripple occurrence. Mean theta and alpha power differed across conditions, whereas the delta– and high-gamma–ripple relationships also varied according to cognitive condition. The estimated delta–ripple slope was greatest under the Calm condition, although the Calm-versus-Free slope difference did not reach nominal significance, whereas the negative high-gamma–ripple relationship observed under the Free condition was significantly altered under the Calculation condition.

Subjective reports linked reduced feedback monitoring and calmer strategies to increased ripple expression

Because categorical task labels provide only an approximate description of participants' ongoing mental states, we complemented the condition-based analyses with a quantitative analysis of post-block free-text reports. Participants described their experiences during each neurofeedback block and the strategies they perceived as increasing or decreasing the feedback signal. These reports were quantified along ten cognitive dimensions using a fixed large language model pipeline blinded to the ripple rates and participant identities (Methods).

We first asked which subjective features covaried with ripple occurrence across 27 participant–condition observations from nine participants. Greater monitoring of the feedback signal was associated with substantially lower ripple rates (β = −2.71 events min^{-1} per 1-SD increase in score, 95% CI − 4.21 to − 1.21, P = 0.0011, FDR-adjusted P = 0.0108; Fig. 3e). Interoceptive attention showed a nominal positive association with the ripple rate (β = 2.37, P = 0.020), whereas task relatedness showed a nominal negative association with the ripple rate (β = −1.78, P = 0.033); however, neither association remained significant after FDR correction (FDR-adjusted P = 0.102 and 0.111, respectively).

We next explored the subjective characteristics of strategies perceived as increasing or decreasing the feedback signal. In linear mixed-effects models with strategy direction as a fixed effect and participant as a random intercept, strategies reported to increase feedback were rated as calmer (β[Increase − Decrease] = 24.98, 95% CI 8.03–41.93, P = 0.0055; Fig. 3f), with more positive valence (β = 17.69, 95% CI 3.68–31.71, P = 0.0156; Fig. 3g) and lower arousal (β = −18.52, 95% CI − 33.22 to − 3.81, P = 0.0156; Fig. 3h). The results for all ten dimensions are shown in Supplementary Fig. 11.

Together, reduced active feedback monitoring was the most robust subjective correlate of the ripple rate, whereas strategies that were reported to increase the feedback signal were characterized by a calmer profile with more positive valence and reduced arousal. Thus, trial-to-trial differences in the subjective cognitive state provided information about ripple expression beyond that conveyed by categorical condition labels.

Discussion

Using real-time visual neurofeedback, we identified cognitive contexts associated with increased expression of waking human hippocampal ripples. Relative to that in a condition without neurofeedback, the ripple rate increased during free-thought neurofeedback and increased further when participants adopted calm strategies, whereas a comparable increase was not observed in a state characterized by continuous mental calculations. Cortical analyses further revealed that the relationship between ongoing spectral activity and ripple expression differed across cognitive conditions, whereas subjective analyses revealed that reduced active monitoring of the feedback signal was the most robust cognitive correlate

of higher ripple rates. Taken together, these findings suggest that hippocampal ripple expression is not uniform across wakefulness states but varies systematically with ongoing cognitive states.

This state dependence extends previous evidence that waking hippocampal ripples occur more frequently during naturally occurring self-generated thought, particularly when cognition is less tightly coupled to an external task[13]. Our condition comparisons are broadly consistent with this account. Ripple rates were higher under the Calm condition than under either the Free or Calculation conditions, and a similarly increased ripple rate was observed under the Meditation condition in the subset of individuals who participated in this condition. However, because the Meditation condition was performed by only six participants, this observation should be considered supportive rather than confirmatory evidence. The lower ripple expression observed under the Calculation condition further suggests that neurofeedback exposure and sustained cognitive effort alone are not sufficient to account for the observed increases. Together, these findings are consistent with the possibility that reduced external constraints favor waking ripple expression. However, because internal orientation was not directly quantified, the present data do not establish that internal orientation itself was the critical factor.

The cortical results suggest that cognitive context was reflected both in mean spectral activity and in the relationship between the cortical network state and hippocampal ripple occurrence. Mean theta and alpha power differed across conditions, whereas no significant condition effects were detected for mean delta or high-gamma power. Nevertheless, both delta– and high-gamma–ripple relationships varied significantly across cognitive conditions. The estimated delta–ripple slope was greatest under the Calm condition, although its difference from that under Free did not reach nominal significance, whereas the negative high-gamma–ripple relationship observed under Free was significantly altered under Calculation. Thus, condition-dependent cortical–hippocampal coupling cannot be explained solely by condition-wide changes in mean spectral power.

This interpretation is consistent with the well-established state dependence of sharp-wave ripples, which preferentially occur during quiescent periods but also support memory-related processing during wakefulness states[2,3,15]. Moreover, hippocampal–cortical coordination during ripple occurrence differs across behavioral states[16,17]. The stronger low-frequency–ripple coupling observed under the Calm condition may therefore reflect a network configuration that is more permissive for intrinsic hippocampal activity, whereas the altered gamma–ripple relationship observed under the Calculation condition may reflect task-related cortical engagement[18,19].

More broadly, hippocampal networks contribute to episodic simulation and the flexible generation of internal representations[20,21]. Thus, cognitive states that support ripple expression may also support the reinstatement or recombination of memory representations. However, creativity, insight and memory recombination were not measured directly in the present study, and any connection between elevated ripple expression and these higher-order cognitive processes remains speculative (Supplementary Fig. 12).

The role of neurofeedback must be considered in interpreting these results. We do not take the observed increases in the ripple rate as evidence that participants acquired direct volitional control over individual ripple events. Rather, neurofeedback provided an evaluative signal through which participants could vary their mental strategies and explore the cognitive states associated with different levels of ripple expression. Neurofeedback generally provides information about ongoing neural activity that can support the discovery and refinement of strategies for neural self-regulation[14]. The present findings reveal an informative tension within this framework: participants were given the explicit external goal of enlarging the feedback circle, yet higher ripple rates were associated with reduced monitoring of that feedback and with calmer subjective states. These observations are not necessarily contradictory. This feedback may have defined the overall objective while functioning intermittently as a cue for evaluating candidate mental states rather than as a signal requiring continuous attentional control. Consistent with this interpretation, greater feedback monitoring was associated with lower ripple expression. Thus, rather than serving as a target for continuous effortful control, the feedback may have served as an intermittent signal that enabled participants to discover the cognitive states in which ripples were more likely to occur.

The temporal evolution of ripple expression provides additional support for an interpretation based on gradual state exploration rather than an immediate response to the onset of neurofeedback. Across early–late boundaries ranging from 1 to 5 min, consistently higher ripple rates were observed during the later portion of the Calm block, with later/early rate ratios greater than 1 for all five boundaries and four of the five comparisons remaining significant after FDR correction. In contrast, the evidence supported a later increase under the Free condition only when the first minute was used as the early period, whereas no significant difference in the later/early rate ratio was observed at any boundary under the Calculation condition. Therefore, the most consistent evidence of a progressive within-block increase in ripple occurrence was observed under the Calm condition. However, because the Poisson mixed-effects model did not yield a significant condition-by-time interaction, these analyses do not establish that the temporal increase itself was significantly greater under the Calm condition than during the other conditions.

The main condition effects were also broadly consistent across individuals and robust to a more stringent definition of hippocampal ripples. The ripple rates of eight of the nine participants increased under the Calm condition relative to that at baseline, and the ripple rates increased under the Calm condition relative to that during Free neurofeedback in seven of the nine participants. This condition-dependent pattern was preserved when the analysis was restricted from all candidate events to a more stringently defined set of high-confidence hippocampal ripple events. This sensitivity analysis is particularly relevant for intracranial recordings from patients with epilepsy, in whom physiological and pathological ripple-band events can overlap in terms of frequency and morphology and cannot be distinguished with absolute certainty[22–25]. We reduced the influence of clearly pathological high-frequency activity by excluding events occurring near interictal epileptiform discharges and applying stringent criteria based on oscillatory morphology and event characteristics. Because these high-confidence events were nested within the full candidate-event set, this analysis should be interpreted as

a test of robustness to the stringency of the event definition rather than as an independent replication of the above results. Nevertheless, the persistence of the principal condition effects under stricter event selection criteria indicates that the findings did not depend on a single detection criterion or readily identifiable epileptiform high-frequency events.

The free-text analyses provided a complementary view of within-condition variations in participants' subjective cognitive states. Reports were quantified using a fixed language model prompt without access to the participant identities, condition labels, ripple rates or other neurophysiological outcomes. After accounting for the cognitive condition, reduced monitoring of the feedback signal remained the strongest subjective correlate of higher ripple rates. In separate exploratory analyses of strategies that participants associated with perceived increases or decreases in the feedback signal, strategies associated with increases in the feedback signal tended to be described as calmer, with a more positive valence and reduced arousal, although these differences did not remain significant after correction across all ten cognitive dimensions. Taken together, these findings suggest that categorical task instructions captured only part of the cognitive variation associated with ripple expression, with additional variability reflected in participants' moment-to-moment or strategy-related subjective states.

Several limitations should be considered. First, although ripple expression was compared with a baseline condition without neurofeedback, sham and yoked-feedback control conditions were not included, and a fully factorial design combining feedback with each cognitive condition was not employed. We therefore cannot completely separate neurofeedback-specific effects from those associated with the cognitive condition or elapsed experimental time. Accordingly, our conclusions are limited to showing that during neurofeedback-guided state exploration, calmer and less task-engaged cognitive states were associated with higher hippocampal ripple expression.

Second, although the direction of the principal effects was consistent across most participants, only nine individuals were included in this study. Replication in larger and more diverse cohorts is needed to establish the robustness and generalizability of these findings.

Third, all participants underwent intracranial electrode implantation for clinical indications, and we cannot completely exclude the possibility that some detected events reflected high-frequency pathological activity. We reduced this risk by excluding events occurring near interictal epileptiform discharges, applying stringent ripple-selection criteria and examining waveform and spectral characteristics. The persistence of the main effects in the high-confidence event subset supports their robustness to the stringency of the event definition but does not eliminate the possibility of residual pathological contamination. Thus, the generalization of these results beyond patients undergoing intracranial monitoring should be performed cautiously.

Finally, free-text reports were obtained after the neurofeedback sessions and therefore did not provide a time-resolved measure of the cognitive state during each session. In addition, although the reports were scored using a fixed language model and prompt to ensure consistency, the resulting cognitive dimensions may still depend on the particular model, prompt formulation, and scoring procedure used.

In conclusion, in this study, using real-time intracranial neurofeedback, we identified cognitive contexts associated with increased expression of waking human hippocampal ripples. Ripple occurrence was highest during instructed relaxation and was accompanied by reduced active feedback monitoring and condition-dependent coupling with cortical spectral activity. These findings show that waking hippocampal ripple expression varies systematically with the cognitive context and provide an experimental framework for probing the brain states associated with endogenous hippocampal dynamics in humans.

Methods

Study design

In this study, real-time visual neurofeedback of human hippocampal ripples in patients undergoing intracranial EEG monitoring for drug-resistant epilepsy was used. Hippocampal ripples were detected online and translated into visual feedback, enabling participants to test different cognitive strategies while receiving feedback related to ongoing ripple occurrence.

The primary experiment included nine participants who performed ripple neurofeedback under different cognitive conditions, namely, Free, Calm and Calculation; six of the nine participants also completed a Meditation condition. We analyzed ripple occurrence and event characteristics, the temporal evolution of ripple occurrence during neurofeedback, participants' subjective reports, and simultaneously recorded cortical activity to characterize the cognitive and neurophysiological features associated with ripple expression.

Participants

Participants were recruited from patients undergoing intracranial EEG monitoring for clinical evaluation of drug-resistant epilepsy. Inclusion required stable electrophysiological recordings from the hippocampus and sufficient cognitive and behavioral capacity to understand and complete the experimental tasks.

The participants' age decades, hippocampal electrode implantation side, duration of intracranial monitoring and electrodes included in the analyses are summarized in Supplementary Table.

Ethics

All participants were recruited from patients undergoing intracranial electrode monitoring at two university hospitals, Osaka University Hospital and Juntendo University Hospital. The study was conducted in accordance with protocols approved by the institutional ethics committees at each site (Osaka University Hospital, approval no. 14353; Juntendo University Hospital, approval no. C24-0138). All participants provided written informed consent before participation.

The locations and duration of intracranial electrode implantation were determined solely on the basis of clinical requirements. No additional electrodes were implanted, and the monitoring period was not extended for research purposes.

Intracranial EEG recording and electrode localization

Intracranial EEG was recorded from subdural and depth electrodes at a sampling rate of 10 kHz using an EEG-1200 system (Nihon Kohden, Tokyo, Japan). Signals were acquired with high-pass and low-pass filters with settings of 0.016 Hz and 3,000 Hz, respectively. For offline analyses, the data were downsampled to 2 kHz after the application of an eighth-order Chebyshev type I low-pass antialiasing filter.

Subdural electrodes were arranged in grid or strip configurations, with an intercontact spacing of 10 mm and a contact diameter of 3 mm at Osaka University. The depth electrodes used at Osaka University had an intercontact spacing of 5–15 mm and a contact length of 1 mm. At Juntendo University, six-contact platinum depth electrodes were used, with a contact length of 2.41 mm and a center-to-center distance of 10 mm. Electrode locations were determined by coregistering postoperative computed tomography images to preoperative T1-weighted magnetic resonance images using FreeSurfer (Boston, MA, USA). Contacts located within or immediately adjacent to the hippocampus and providing stable local electrophysiological signals were considered candidate contacts for online hippocampal ripple detection. The electrode locations were reconstructed in each participant's native anatomical space and labeled using FreeSurfer aparc+aseg. The contacts were assigned their corresponding anatomical labels. Contacts localized to white matter were assigned to the nearest cortical region.

Real-time ripple detection and visual neurofeedback

Intracranial EEG signals from a bipolar hippocampal channel formed from two hippocampal contacts were used for neurofeedback. The signals were rereferenced online in a bipolar configuration and then entered into the real-time ripple detection algorithm. For online ripple detection, the bipolar signal was bandpass filtered at 70–180 Hz, and root-mean-square (RMS) amplitudes were calculated continuously using a short time window of 8 ms and a long time window of 2,000 ms. A ripple event was detected when the ratio of the short-window RMS to the long-window RMS (*RMS (8 ms)/RMS (2,000 ms)*) exceeded 2 continuously for at least 8 ms. These detection parameters were held constant across all the neurofeedback sessions. The visual feedback value was calculated from the online ripple-detection output during the 10-s period preceding each feedback update. Specifically, the detection output within each 10-s window was summed and added to a predefined baseline to obtain the display value. This value was clipped to a predefined display range, linearly rescaled to an integer between 0 and 255, and transmitted to the visual feedback system. The participants viewed a circle whose size varied in real time as a function of this feedback value. During each feedback update, the raw online detection output, display value before clipping, clipped value and final feedback value presented to the participant were stored for subsequent analyses. The detection criteria used for online neurofeedback were defined independently from those used for offline ripple analyses of the stored intracranial EEG recordings.

Participants were instructed to modify their thoughts or attentional state with the aim of increasing the visual feedback signal. They were not provided with detailed information about the physiological significance of hippocampal ripples beyond that necessary to perform the neurofeedback task.

Cognitive conditions

The neurofeedback experiment included several cognitive conditions. In the Free condition, participants were not assigned a specific cognitive task and were instructed to think freely. No restrictions were imposed on the thought content or the strategies used. In the Calm condition, participants were instructed to relax their body and maintain a calm mental state. The specific thought content was not otherwise constrained. In the Calculation condition, participants performed continuous mental arithmetic consisting of serial subtraction. Task difficulty was adjusted individually so that participants could sustain performance throughout the session. In the Meditation condition, participants were instructed to direct their attention toward their breathing, bodily sensations or current internal state while minimizing engagement with ongoing thoughts. Each neurofeedback condition lasted 10 min. The timing of individual sessions varied according to the clinical schedule and the participant's condition.

Offline detection of hippocampal ripple events

After the neurofeedback experiment was complete, hippocampal ripple events were detected offline from the stored intracranial EEG recordings. Offline detection was performed on bipolar hippocampal signals filtered at 80–250 Hz. Interictal epileptiform discharges (IEDs) were independently detected from the two constituent monopolar contacts in the 20–80-Hz band, and candidate ripple events occurring within ± 0.5 s of an IED detected in either contact were excluded. Periods of global high-frequency noise were also excluded from ripple detection. Candidate events were identified using start/end and peak amplitude thresholds of 2 and 5 standard deviations, respectively, with durations of 30–200 ms; events separated by less than 30 ms were merged. High-confidence ripple events were also required to exhibit a spectral peak between 60 and 180 Hz, a log spectral prominence of at least 0.2, and at least three oscillatory cycles.

Two nested event sets were used for subsequent analyses. The ALL event set comprised candidate high-frequency events satisfying the primary amplitude, duration and artifact exclusion criteria, whereas the high-confidence (HC) event set also required features intended to increase specificity for oscillatory ripple events, including narrowband spectral structures and multiple oscillatory cycles[26]. Because the high-confidence events constituted a subset of the ALL event set, analyses using the two definitions were interpreted as sensitivity analyses assessing robustness to the stringency of the ripple classification criteria rather than as independent replications of the results.

Ripple rate and event characteristics

The ripple rate was calculated as the number of valid ripple events divided by the valid analyzed recording time and expressed as the number of events per minute. Periods that were excluded because of interictal epileptiform activity or noise were removed from the denominator. For the no-neurofeedback

baseline, we used the 30-s period immediately preceding the start of each Free, Calculation and Calm neurofeedback block. For each participant, the ripple counts and valid recording times were pooled across these baseline periods, and the baseline ripple rate was calculated as the total number of events divided by the total valid duration of the baseline period. Baseline periods preceding Meditation blocks were not included to ensure that the baseline definition was identical across all nine participants.

Primary analyses of ripple occurrence were performed using the ALL event set. Ripple counts were analyzed using Poisson generalized linear mixed-effects models with a log link, the participant as a random intercept and the logarithm of the valid recording time in minutes as an offset. Ripple occurrence during the baseline period was compared separately with that during the Free, Calculation, Calm and Meditation periods using participants for whom both observations were available. The P values for these four baseline comparisons were adjusted using the Benjamini–Hochberg FDR procedure. Direct comparisons among the Free, Calculation, Calm and Meditation conditions were performed using the same exposure-adjusted Poisson mixed-effects framework, with FDR correction applied across the six pairwise condition comparisons. The Meditation condition was performed by six participants; missing observations were not imputed. To assess whether baseline-to-condition effects were disproportionately influenced by individual participants, the Poisson models were repeated after each participant was excluded in turn in leave-one-participant-out analyses.

Event characteristics were examined separately from the ripple occurrence rate and were treated as exploratory analyses. For each participant and condition, the ripple peak amplitude was summarized using the mean event-wise ripple-band amplitude-envelope measure, the peak frequency was summarized using the mean event-wise peak frequency, and the ripple duration was summarized using the median event duration. These analyses included only the four neurofeedback conditions—Free, Calculation, Calm and Meditation—and did not include the baseline periods. Condition differences were evaluated using paired Wilcoxon signed-rank tests for all available condition pairs, with Benjamini–Hochberg FDR correction applied across the six pairwise comparisons separately for each ripple characteristic. Participant-level summaries, rather than individual ripple events, were used as the statistical unit to avoid event-level pseudoreplication.

All analyses were repeated using the HC event set as a sensitivity analysis. HC events comprised a subset of the ALL event set that satisfied more stringent criteria for oscillatory morphology. Because the HC set was nested within the ALL set, these analyses were interpreted as tests of robustness to the stringency of the ripple definition rather than as independent replication of the results.

Temporal analysis

To characterize within-block temporal evolution, the neurofeedback sessions were divided into consecutive 2-min bins. Across the Free, Calculation and Calm conditions, ripple counts were analyzed using an exposure-adjusted Poisson mixed-effects model including the condition, continuous time and their interaction, with participant-specific random effects and the logarithm of the valid recording time as an offset. To explore nonlinear early-versus-later differences without prespecifying a transition point,

each block was additionally divided using boundaries from 1 to 5 min, and later/early rate ratios were estimated separately within each condition. Benjamini–Hochberg FDR correction was applied across the five alternative boundaries within each condition. Because the Meditation condition was available for only six participants, its temporal profile was treated descriptively.

Cumulative distribution of cortical delta activity during ripple events

To characterize the cortical delta state at the time of ripple occurrence, delta band power was sampled at the peak of each detected ripple event. For each participant, delta power was standardized relative to the distribution of valid cortical delta activity pooled across the Free, Calculation, and Calm conditions, yielding participant-specific z scored delta values.

The empirical cumulative distribution function of delta power during ripple events was then calculated separately for each participant. To avoid disproportionate weighting of participants with more detected events, participant-level cumulative distributions were averaged across participants with equal weighting. The cumulative distributions were evaluated over a common delta-power grid spanning the 1st to 99th percentiles of the pooled event-related delta values. The Free, Calculation, and Calm conditions were pooled for this analysis.

Cortical spectral analysis

To characterize cortical activity associated with hippocampal ripple expression, intracranial EEG signals recorded from nonhippocampal cortical electrodes were analyzed in the frequency domain. Analyses were restricted to the predefined analysis interval for each recording, and time points identified as artifacts were excluded.

Cortical electrodes were identified on the basis of anatomical location. Spectral power was quantified in six frequency bands: delta (1–4 Hz), theta (4–8 Hz), alpha (8–13 Hz), beta (13–30 Hz), low gamma (30–60 Hz), and high gamma (70–150 Hz). After line noise removal, the signals were bandpass filtered within each frequency range, and the instantaneous power was obtained from the squared magnitude of the analytic signal derived using the Hilbert transform. Power was expressed in decibels (10 × log10[power]). Band-specific power was first calculated separately for each cortical contact and subsequently averaged across cortical contacts within each participant and recording.

The mean cortical band power was compared among the Free, Calculation, and Calm conditions using linear mixed-effects models with condition as a fixed effect and participant as a random intercept as follows: Band power ~ Condition + (1 | Participant).

To examine whether ongoing fluctuations in cortical spectral activity were associated with ripple occurrence, each recording was divided into 60-s windows. For each valid window, the mean cortical band power and ripple rate were calculated. Band-power values were standardized within each participant.

For each frequency band, the association between the cortical power and ripple rate was first assessed using a linear mixed-effects model including condition as a covariate: Ripple rate ~ Band power (z) + Condition + (1 | Participant).

To determine whether the relationship between cortical activity and ripple occurrence differed according to the cognitive condition, an interaction model was also fitted: Ripple rate ~ Band power (z) × Condition + (1 | Participant).

The interaction was evaluated by a likelihood ratio comparison of the interaction model with the corresponding additive model.

Collection of subjective reports

After each neurofeedback session, participants were asked verbally to describe what they had been thinking or experiencing during the neurofeedback session. They were also asked what they had been thinking or doing when they perceived the feedback signal as becoming larger or smaller.

When no corresponding description was provided, the relevant increase- or decrease-associated category was treated as absent. Importantly, decrease-associated reports reflected cognitive states or strategies that participants associated with a reduction in the feedback signal and did not imply that participants had intentionally attempted to decrease the signal.

Quantification of subjective reports using a large language model

Free-text reports were quantitatively characterized using GPT-5 (OpenAI) through the OpenAI Responses API. Reports were scored along ten cognitive dimensions: interoceptive attention, task relatedness, calmness, effortfulness, feedback monitoring, memory/past orientation, future orientation, imagery, positive valence and arousal.

Each report was evaluated separately across three categories: during-NF experience, increase-associated strategy and decrease-associated strategy. The during-NF experience category was scored on a 1–100 scale for each cognitive dimension. For the increase- and decrease-associated strategies that were available, the scores ranged from 0 to 100. Scores of 0 were treated as missing values and excluded from the statistical analyses. When no increase- or decrease-associated description was available, that strategy category was treated as missing and excluded from the corresponding strategy analysis.

The prompt provided operational definitions for each cognitive dimension, the scoring criteria, the extraction of the supporting text and the required structured-output format. The language model was provided with only the participants' reports and was not provided the participant identifiers, experimental condition labels, ripple rates or other neurophysiological outcomes. The complete prompts are provided in the Supplementary Method.

Association between the LLM-derived cognitive scores and the ripple rate

For the during-NF experience analysis, the LLM-derived cognitive scores were linked to the corresponding ripple rate for each participant and cognitive condition. Each cognitive dimension was analyzed separately using a linear mixed-effects model with the following form:

Ripple rate ~ standardized cognitive score + condition + (1 | participant).

The ripple rate was the dependent variable, and the z-standardized cognitive score was the primary fixed-effect predictor. The cognitive condition was included as an additional fixed effect to account for condition-level differences in both the subjective state and ripple expression, and participants were included as a random intercept to account for interindividual differences in the baseline ripple rate.

For each cognitive dimension, we estimated the fixed-effect coefficient, standard error, 95% confidence interval and P value. To account for testing across multiple cognitive dimensions, P values were adjusted using the Benjamini–Hochberg FDR procedure.

Comparison of increase- and decrease-associated reports

To characterize the cognitive features associated with strategies that participants perceived as increasing or decreasing the feedback signal, we compared LLM-derived scores from increase-associated and decrease-associated reports. Each of the ten cognitive dimensions was analyzed separately using a linear mixed-effects model with strategy direction as a fixed effect and participants as a random intercept:

cognitive score ~ strategy direction + (1 | participant).

Decrease-associated reports served as the reference category; thus, the coefficient for the strategy direction represented the estimated difference in the score between the increase- and decrease-associated reports (Increase − Decrease), with positive values indicating higher scores for increase-associated strategies. Benjamini–Hochberg FDR correction was applied across the ten cognitive dimensions.

The cognitive condition was intentionally omitted from these models because the analysis was designed to characterize subjective features that distinguished perceived increase-associated and decrease-associated strategies across conditions rather than to estimate condition-adjusted strategy effects.

Statistical analysis

Statistical analyses were performed using MATLAB R2023a (MathWorks, Natick, MA, USA).

Mixed-effects models were used for analyses involving repeated observations within participants. In the ripple-count analyses, Poisson generalized linear mixed-effects models with a log link and the logarithm

of the valid recording time as an offset were used, with the participant included as a random effect, as specified for each analysis. Continuous outcomes were analyzed using linear mixed-effects models where indicated. In the analyses of the strategy direction of the LLM-derived scores, linear mixed-effects models with the participant as a random intercept were used.

P values were adjusted for multiple comparisons as specified for each analysis, primarily using the Benjamini–Hochberg FDR procedure; the Holm correction was used for pairwise comparisons of the magnitude of the displayed neurofeedback. Tests of fixed-effect coefficients and pairwise contrasts were two-sided. Unadjusted P values < 0.05 were considered nominally significant, whereas adjusted P values < 0.05 were considered statistically significant after correction for multiple comparisons. Effect estimates are reported, where appropriate, as fixed-effect coefficients, rate ratios, or paired differences together with 95% confidence intervals.

Condition order and blinding

The Free condition was generally performed first. The order of the remaining cognitive conditions was not randomized or fixed in advance and varied across participants according to experimental and clinical circumstances.

The participants were instructed to modulate their thoughts or attentional state to increase the visual feedback signal but were not given detailed information regarding the physiological significance of hippocampal ripples beyond that required to perform the task.

The offline ripple detection was performed using a predefined automated algorithm. Artifact and interictal epileptiform-discharge inspections were performed without access to the neurofeedback results or the participant-level ripple-rate outcomes, and the evaluators were blinded to cognitive condition. For the free-text analysis, the language model was provided with only the participants' reports and was not provided the participant identifiers, experimental condition labels, ripple rates, or other neurophysiological outcomes.

Use of generative AI

Generative AI tools, specifically ChatGPT (OpenAI), were used to assist with English-language editing and the development and debugging of portions of the analysis code. All AI-assisted text and code were reviewed, edited and validated by the authors before use. The authors take full responsibility for the accuracy of the analyses, interpretation of the results and content of the manuscript.

Declarations

Data availability

Public release of the complete raw intracranial EEG datasets is restricted because these recordings contain potentially identifiable clinical information. Deidentified data supporting the findings of this

study, including ripple-event timings and analysis tables, will be made available within the constraints of applicable ethical and legal requirements.

Code availability

The code used for the principal ripple detection and statistical analyses will be made publicly available upon publication.

Acknowledgments

We thank Maiko Okamura for their assistance with data collection.

Funding

This work was supported by the Japan Science and Technology Agency (JST) Moonshot R &D-MILLENNIA Program (JPMJMS2012), the JST K Program (grant no. JPMJKP25Y7), the Japan Agency for Medical Research and Development (AMED) (grant no. JP24wm0625207), the Sumino Isamu Foundation, the Japan Epilepsy Research Foundation (JERF) (grant no. JERF TENKAN 25003), the Brain Science Foundation, and the Narishige Neuroscience Research Foundation.

Author contributions

T.I.: Conceptualization, Data curation, Formal analysis, Funding acquisition, Investigation, Methodology, Visualization, Writing – original draft, Writing – review & editing.

T.Y.: Conceptualization, Funding acquisition, Methodology, Project administration, Supervision, Writing – review & editing.

Yu.I.: Conceptualization, Investigation, Methodology, Supervision, Writing – review & editing.

R.F.: Investigation, Data curation, Software, Writing – review & editing.

S.O.: Investigation, Resources, Data curation.

N.T.: Investigation, Resources, Data curation.

Hu.K.: Investigation, Resources, Data curation.

Ya.I.: Investigation, Resources, Data curation.

H.S.: Investigation, Resources, Data curation.

T.M.: Investigation, Resources, Data curation.

Ha.K.: Investigation, Resources, Data curation, Project administration.

Competing interests

The authors declare that they have no competing interests.

References

1. Buzsáki G (2015) Hippocampal sharp wave-ripple: A cognitive biomarker for episodic memory and planning. Hippocampus 25:1073–1188
2. Joo HR, Frank LM (2018) The hippocampal sharp wave-ripple in memory retrieval for immediate use and consolidation. Nat Rev Neurosci 19:744–757
3. Jadhav SP, Kemere C, German PW, Frank LM (2012) Awake hippocampal sharp-wave ripples support spatial memory. Science 336:1454–1458
4. Vaz AP, Inati SK, Brunel N, Zaghloul KA (2019) Coupled ripple oscillations between the medial temporal lobe and neocortex retrieve human memory. Science 363:975–978
5. Norman Y et al (2019) Hippocampal sharp-wave ripples linked to visual episodic recollection in humans. Science 365
6. Kerrén C, Michelmann S, Doeller CF (2026) Hippocampal ripples initiate cortical dimensionality expansion for memory retrieval. Nat Commun 17
7. He L et al (2026) Human hippocampal ripples coordinate planning sequences and compositional representations in neocortex. Nat Neurosci 29:1711–1721
8. Foster DJ, Wilson MA (2006) Reverse replay of behavioural sequences in hippocampal place cells during the awake state. Nature 440:680–683
9. Pfeiffer BE, Foster DJ (2013) Hippocampal place-cell sequences depict future paths to remembered goals. Nature 497:74–79
10. Smallwood J, Schooler JW (2015) The science of mind wandering: empirically navigating the stream of consciousness. Annu Rev Psychol 66:487–518
11. Christoff K, Irving ZC, Fox KCR, Spreng RN, Andrews-Hanna JR (2016) Mind-wandering as spontaneous thought: a dynamic framework. Nat Rev Neurosci 17:718–731
12. Smallwood J (2013) Distinguishing how from why the mind wanders: a process-occurrence framework for self-generated mental activity. Psychol Bull 139:519–535
13. Iwata T et al (2024) Hippocampal sharp-wave ripples correlate with periods of naturally occurring self-generated thoughts in humans. Nat Commun 15:4078
14. Sitaram R et al (2017) Closed-loop brain training: the science of neurofeedback. Nat Rev Neurosci 18:86–100
15. Roumis DK, Frank LM (2015) Hippocampal sharp-wave ripples in waking and sleeping states. Curr Opin Neurobiol 35:6–12
16. Tang W, Shin JD, Frank LM, Jadhav SP (2017) Hippocampal-Prefrontal Reactivation during Learning Is Stronger in Awake Compared with Sleep States. J Neurosci 37:11789–11805

17. Remondes M, Wilson MA (2015) Slow-γ Rhythms Coordinate Cingulate Cortical Responses to Hippocampal Sharp-Wave Ripples during Wakefulness. Cell Rep 13:1327–1335
18. Meltzer JA et al (2008) Effects of working memory load on oscillatory power in human intracranial EEG. Cereb Cortex 18:1843–1855
19. Jerbi K et al (2009) Task-related gamma-band dynamics from an intracerebral perspective: review and implications for surface EEG and MEG. Hum Brain Mapp 30:1758–1771
20. Thakral PP, Madore KP, Kalinowski SE, Schacter DL (2020) Modulation of hippocampal brain networks produces changes in episodic simulation and divergent thinking. *Proc. Natl. Acad. Sci. U. S. A.*117, 12729–12740
21. Addis DR, Pan L, Vu M-A, Laiser N, Schacter DL (2009) Constructive episodic simulation of the future and the past: distinct subsystems of a core brain network mediate imagining and remembering. Neuropsychologia 47:2222–2238
22. Ye H, Chen C, Weiss SA, Wang S (2024) Pathological and Physiological High-frequency Oscillations on Electroencephalography in Patients with Epilepsy. Neurosci Bull 40:609–620
23. Iwata T et al (2025) Abnormal Synchronization Between Cortical Delta Power and Ripples in Hippocampal Sclerosis. Ann Clin Transl Neurol 12:986–997
24. Iwata T (2026) Pathological and Physiological Significance of Hippocampal Ripples in Epilepsy. JMA J 9:736–741
25. Bruder JC et al (2017) Physiological Ripples Associated with Sleep Spindles Differ in Waveform Morphology from Epileptic Ripples. Int J Neural Syst 27:1750011
26. Maslarova A et al (2025) Spatiotemporal patterns differentiate hippocampal sharp-wave ripples from interictal epileptiform discharges in mice and humans. Nat Commun 16:11636

Figures

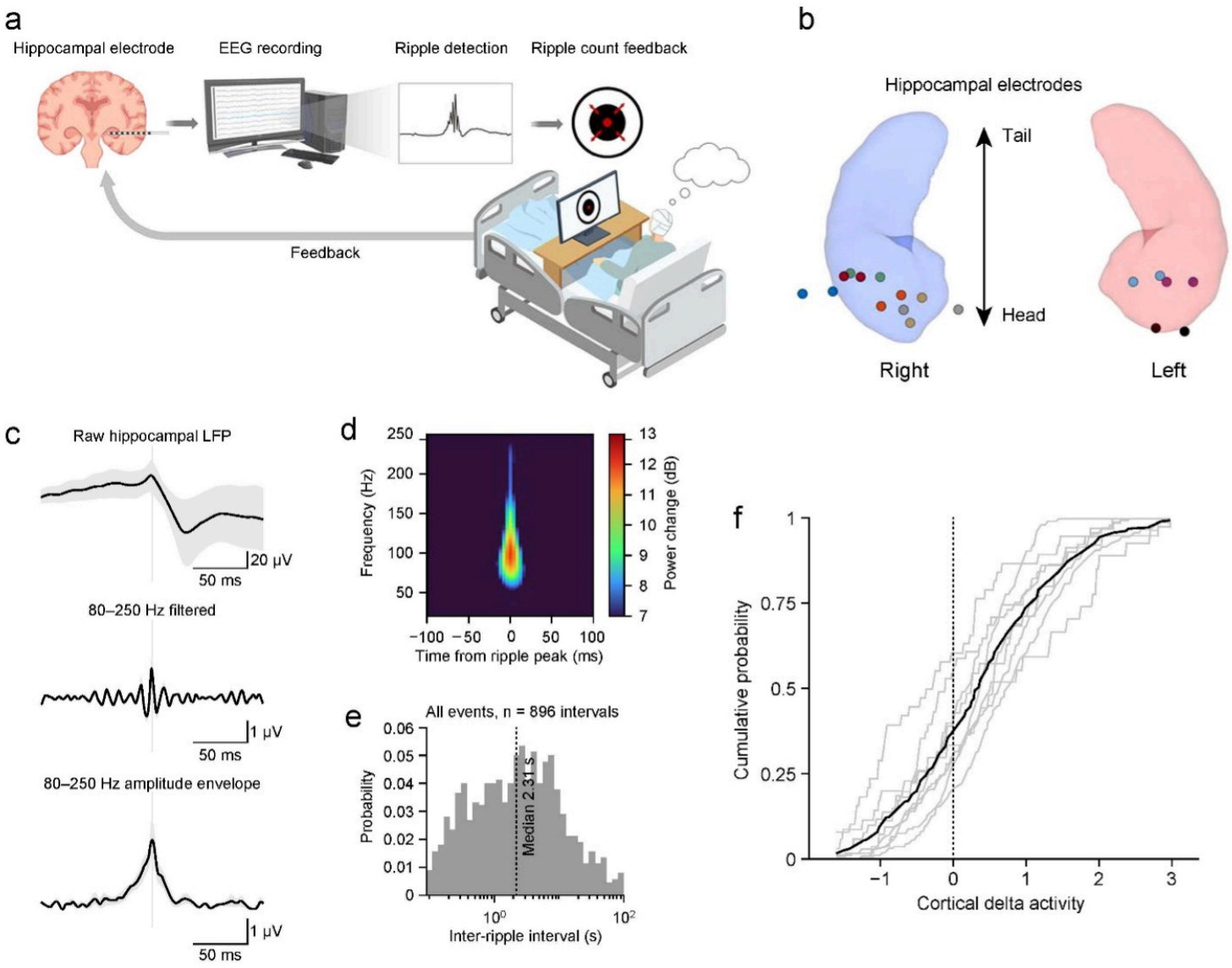


Figure 1

Real-time neurofeedback of human hippocampal ripples.
a, Schematic of the visual neurofeedback (NF) paradigm. Hippocampal electrophysiological activity was recorded from implanted intracranial electrodes, and hippocampal ripples were detected online in real time. Recent ripple occurrence was translated into the size of a visual feedback circle. The participantsvaried their thoughts and mental strategies while attempting to change the size of the circle. b, Locations of the hippocampal electrodes used for online ripple detection in the nine participants, shown on standardized hippocampal surfaces. The electrode contacts are color-coded by participant. The right and left hippocampal surfaces are shown in blue and red, respectively. c, Ripple-centered electrophysiological features of events identified during NF by offline analysis using the ALL event definition. Top, participant-averaged raw hippocampal local field potential (LFP) aligned to the ripple peak; middle, participant-averaged ripple-band-filtered signal (80–250 Hz); bottom, participant-averaged amplitude envelope of the ripple-band-filtered signal. The solidlines indicate the mean across participants (n = 9), with participants weighted equally, and the shaded regions indicate ± s.e.m. Scale

bars are shown in each panel. Across participants, the mean ripple peak frequency was 96.1 ± 10.8 Hz, and the mean ripple duration was 67.2 ± 7.8 ms (mean ± s.d., n = 9). d, Ripple-centered time–frequency representation of hippocampal activity for events in the ALL event set. The x-axis indicates the time from the ripple peak (ms), and the color scale indicates the power (dB). The data were averaged across nine participants. e, Distribution of valid inter-ripple intervals for ALL events identified during NF by the offline analysis. The x-axis shows the inter-ripple interval on a logarithmic scale; n = 896 inter-ripple intervals, with a median interval of 2.31 s. f, Empirical cumulative distribution of cortical delta-band power at the time of ripple occurrence. Cortical delta power was standardized within participants relative to valid cortical activity. The x-axis indicates the standardized cortical delta-band power, and the y-axis indicates the cumulative relative frequency. The gray lines indicate individual participants (n = 9), and the solid line indicates the participant-averaged cumulative distribution.

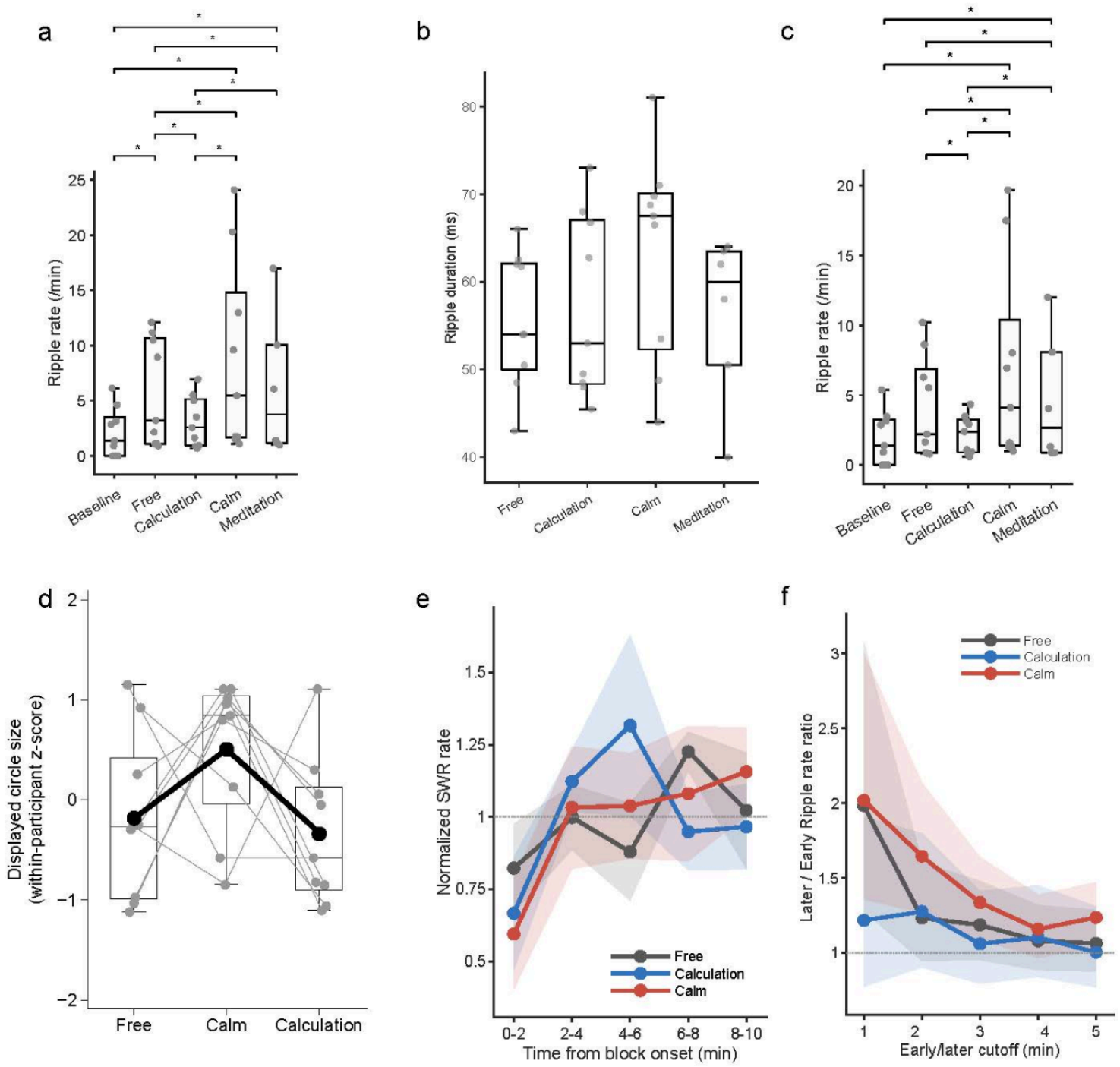


Figure 2

Cognitive-state dependence, robustness, and temporal dynamics of hippocampal ripple expression during neurofeedback.

a, Absolute ripple rates during the no-neurofeedback baseline and the Free, Calculation, Calm and Meditation conditions for the primary ALL event set. Each point represents the ripple rate for one participant, and the box plots summarize the participant-level distributions. Nine individuals participated in the Free, Calculation and Calm conditions; only six individuals participated in the Meditation condition. Statistical inference was performed on the basis of exposure-adjusted Poisson generalized linear mixed-

effects models of ripple counts with participant as a random intercept and valid recording time as an offset. Relative to baseline, the ripple rate was higher under the Free (rate ratio (RR) = 2.15, 95% CI 1.36–3.39, FDR-adjusted P = 0.00355), Calm (RR = 2.91, 95% CI 1.85–4.57, FDR-adjusted P = 5.22×10^{-4}) and Meditation conditions (RR = 3.16, 95% CI 1.75–5.68, FDR-adjusted P = 0.00285), but not under the Calculation condition (RR = 1.13, 95% CI 0.71–1.80, FDR-adjusted P = 0.589). Direct comparisons revealed a higher ripple rate under Calm than under Free (Calm/Free RR = 1.49, 95% CI 1.30–1.71, FDR-adjusted P = 1.59×10^{-5}) and a lower ripple rate under Calculation than under Free (Calculation/Free RR = 0.55, 95% CI 0.46–0.65, FDR-adjusted P = 4.76×10^{-6}).

b, Ripple duration across the four neurofeedback conditions for the ALL event set. Each point represents the participant-level median ripple duration,and the box plots summarize the distributions across participants. Ripple duration was nominally longer under Calm than under Free (median paired difference [Calm − Free], 5.75 ms; two-sided paired Wilcoxon signed-rank test, P = 0.0156) and Meditation (median paired difference [Calm − Meditation], 6.88 ms; P = 0.0313). Neither difference remained significant after FDR correction across the six pairwise condition comparisons (FDR-adjusted P = 0.0938 for both), and no duration comparison remained significant after correction.

c, Absolute ripple rates during the no-neurofeedback baseline and the four neurofeedback conditions using the more stringent high-confidence (HC) ripple definition, displayed as in a. The principal condition-dependent patterns were retained: the ripple rate was higher under Calm than at baseline (RR = 2.50, 95% CI 1.55–4.01, FDR-adjusted P = 0.00347) and higher under Meditation than at baseline (RR = 2.49, 95% CI 1.35–4.58, FDR-adjusted P = 0.0156), whereas the Calculation condition did not differ from baseline (RR = 0.91, 95% CI 0.55–1.49, FDR-adjusted P = 0.686). The ripple rate was higher under Calm than under Free (Calm/Free RR = 1.62, 95% CI 1.38–1.89, FDR-adjusted P = 1.97×10^{-5}), whereas the ripple rate under Calculation was lower than under Free (Calculation/Free RR = 0.55, 95% CI 0.45–0.68, FDR-adjusted P = 2.39×10^{-5}). The baseline-to-Free effect was attenuated and did not survive FDR correction under the HC definition (RR = 1.66, 95% CI 1.03–2.69, nominal P = 0.0402, FDR-adjusted P = 0.0536).

d, Magnitude of the visual feedback signal presented to participants during the Free, Calculation and Calm conditions. Each point represents the participant-level mean feedback value (z score); the box plots summarize the distributions. The blackpoints indicate the group means, and the connecting line links the group means across conditions. The displayed feedback tended to be greater during the Calm condition than during the Calculation condition, although this difference was not statistically significant after correction (Calculation − Calm mean difference = −1.02, 95% CI −2.15 to 0.12; paired t test, t(8) = −2.07, P = 0.072, Holm-adjusted P = 0.217; n = 9).

e, Temporal evolution of the normalized ripple rate during the Free, Calculation and Calm conditions. The ripple rates were calculated in consecutive 2-min bins and normalized within participants. Black, Free; blue, Calculation; red, Calm. The points and solid lines indicate the mean across participants, and the shaded regions indicate ± s.e.m. An exposure-adjusted Poisson mixed-effects model of ripple counts with time, condition and their interaction revealed a significant overall effect of condition (F(2,262) =

14.19, P = 1.41 × 10^{-6}), whereas the main effect of time (F(1,262) = 1.02, P = 0.313) and the condition-by-time interaction (F(2,262) = 1.29, P = 0.277) were not significant.

f, Exploratory analysis of changes in ripple expression between earlier and later portions of each NF block. The early/late boundary was systematically varied from 1 to 5 min after block onset; the x-axis indicates the cutoff, and the y-axis indicates the model-estimated late/earlyripple-rate ratio. Black, Free; blue, Calculation; red, Calm. The points and solid lines indicate the rate ratio estimates from exposure-adjusted Poisson mixed-effects models, and the shaded regions indicate 95% confidence intervals. The horizontal reference line denotes a rate ratio of 1. In the Calm condition, the later/early RR was greater than 1 for all five boundaries (1 min, RR = 2.02, 95% CI 1.36–3.00; 2 min, RR = 1.64, 1.27–2.13; 3 min, RR = 1.34, 1.09–1.64; 4 min, RR = 1.16, 0.97–1.39; 5 min, RR = 1.24, 1.04–1.47), with the 1-, 2-, 3- and 5-min effects remaining significant after FDR correction across the five cutoffs (q = 0.0021, 0.0018, 0.0106 and 0.0225, respectively). In the Free condition, a significant later/early increase was observed only at the 1-min cutoff (RR = 1.98, 95% CI 1.28–3.08, q = 0.0149), whereas no significant effect was observed under the Calculation condition at any cutoff.

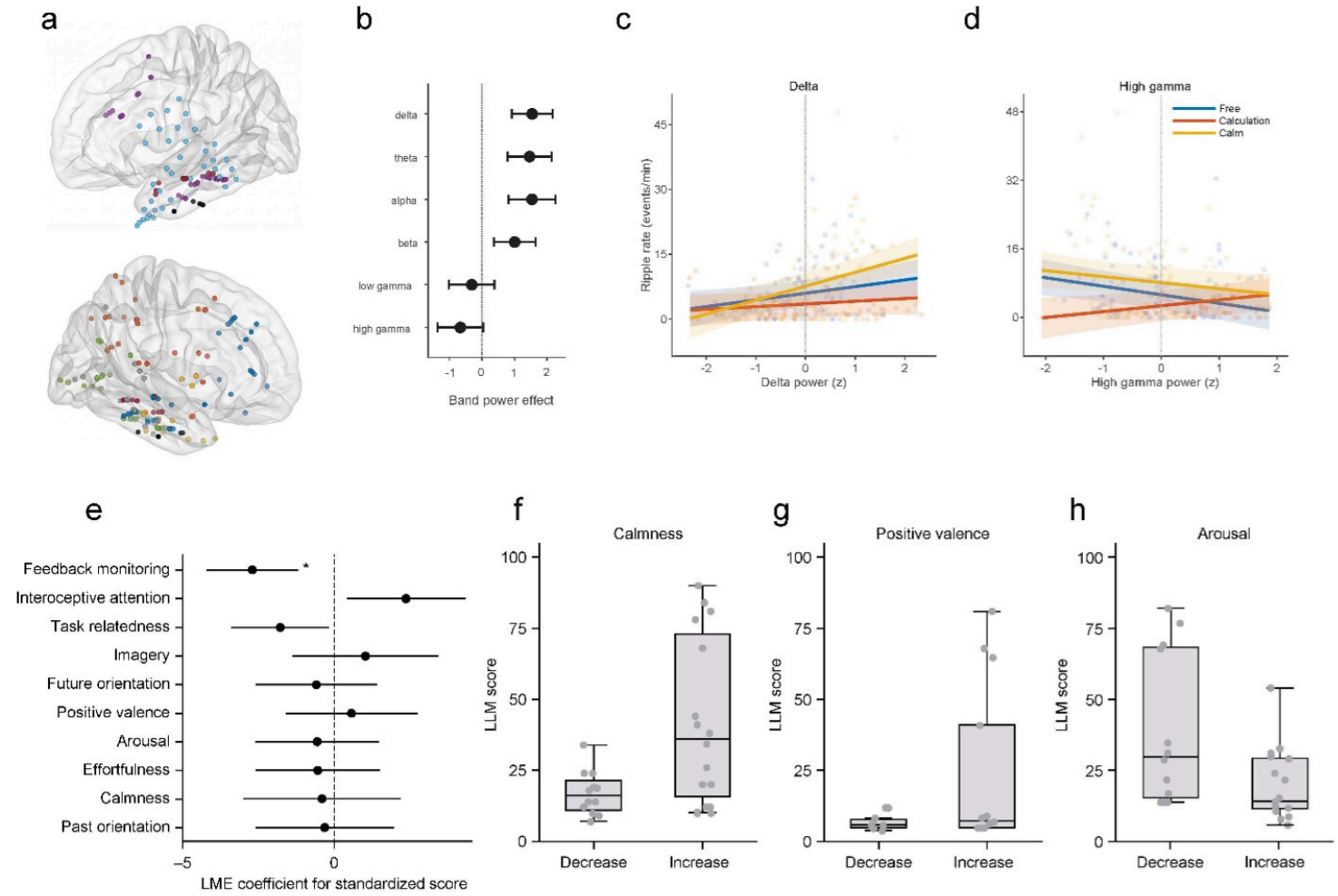


Figure 3

Cortical spectral activity and LLM-derived subjective features associated with hippocampal ripple expression.

a, Locations of cortical electrodes included in the spectral analyses across all participants (n = 9). The electrodes are color-coded by participant. b, Association between the cortical spectral power and ripple rate for the primary ALL event set. Recordings were divided into valid 60-s windows (n = 260 windows from 9 participants), and the standardized band power was related to the ripple rate using separate linear mixed-effects models for each frequency band, with the cognitive condition as a fixed effect and the participant as a random intercept (ripple rate ~ band power (z) + condition + (1 | participant)). The points indicate fixed-effect coefficients for a 1-s.d. increase in band power,and the horizontal lines indicate 95% confidence intervals. The ripple rate was positively associated with delta (β = 1.55 events min^{-1} per s.d., 95% CI 0.92–2.18, q = 1.41×10^{-5}), theta (β = 1.47, 95% CI 0.79–2.14, q = 6.52×10^{-5}), alpha (β = 1.54, 95% CI 0.82–2.26, q = 6.52×10^{-5}) and beta power (β = 1.01, 95% CI 0.37–1.65, q = 0.00335). The associations with low-gamma (β = −0.31, 95% CI −1.01 to 0.39, q = 0.381) and high-gamma power (β = −0.66, 95% CI −1.37 to 0.04, q = 0.0774) did not survive FDR correction.The q values are Benjamini–Hochberg FDR-adjusted values across the six frequency bands. The frequency bands were as follows: delta, 1–4 Hz; theta, 4–8 Hz; alpha, 8–13 Hz; beta, 13–30 Hz; low gamma, 30–60 Hz; and high gamma, 70–150 Hz.

c, Relationship between the standardized cortical delta power and the ripple rate across the Free, Calculation and Calm conditions. The individual points indicate the observed 60-s windows; the solid lines show fixed-effect predictions from the interaction model (ripple rate ~ delta power (z) × condition + (1 | participant)); and the shaded regions indicate 95% confidence intervals. Blue, Free; red, Calculation; yellow, Calm. The delta-power-by-condition interaction was significant (likelihood-ratio $\chi^2(2) = 8.51$, P = 0.0142, q = 0.0284). Under the Free condition, the ripple rate increased with increasing delta power (β = 1.55 events min^{-1} per s.d., 95% CI 0.28–2.81, P = 0.0167). The estimated slope was steeper under the Calm condition (3.23 events min^{-1} per s.d.), although the Calm-by-delta contrast relative to Free did not reach nominal significance (β = 1.68, 95% CI −0.08 to 3.43, P = 0.0606). The slope under the Calculation condition did not differ significantly from that under Free (interaction β = −0.91, 95% CI −2.59 to 0.76, P = 0.283).

d, Relationship between the standardized cortical high-gamma power and the ripple rate, displayed as in c. The high-gamma-power-by-condition interaction was significant (likelihood-ratio $\chi^2(2) = 14.55$, P = 6.91×10^{-4}, q = 0.00415). Under the Free condition, higher high-gamma power was associated with a lower ripple rate (β = −1.99 events min^{-1} per s.d., 95% CI −3.26 to −0.73, P = 0.0021). This relationship differed under the Calculation condition (Calculation × high gamma: β = 3.37 events min^{-1} per s.d., 95% CI 1.53–5.21, P = 3.80×10^{-4}) but not under the Calm condition (Calm × high gamma: β = 0.59 events min^{-1} per s.d., 95% CI −1.31 to 2.49, P = 0.544).

e, Associations between the LLM-derived cognitive features reported after NF and the ripple rate. Free-text reports were quantified along ten cognitive dimensions. Each dimension was analyzed separately using a linear mixed-effects model with the standardized score and condition as fixed effects and the

participant as a random intercept (up to 27 participant–condition observations from 9 participants). The points indicate fixed-effect coefficients for a 1-s.d. increase in score, and the horizontal lines indicate 95% confidence intervals. Greater feedback monitoring was associated with a lower ripple rate (β = −2.71 events min^{-1} per s.d., 95% CI −4.21 to −1.21, P = 0.0011, q = 0.0108) and was the only association that remained significant after FDR correction across the ten dimensions. Interoceptive attention was nominally positively associated with the ripple rate (β = 2.37, 95% CI 0.40–4.33; P = 0.020; q = 0.102), whereas task relatedness was nominally negatively associated with the ripple rate (β = −1.78, 95% CI −3.40 to −0.15; P = 0.033;q = 0.111); neither association survived FDR correction.

f–h, LLM-derived scores for strategies reported by participants as being associated with decreases or increases in the NF signal. The gray points indicate individual strategy reports. The boxes indicate the median and interquartile range, with the whiskers extending to the nonoutlier range. In the statistical comparisons, linear mixed-effects models with the strategy direction as a fixed effect and the participant as a random intercept (score ~ direction + (1 | participant)) were used; the β values represent Increase − Decrease. f, Strategies associated with an increase in the NF signal had higher calmness scores (28 observations from 9 participants; β = 24.98, 95% CI 8.03–41.93; P = 0.0055). g, Strategies associated with an increase in the NF signal had higher positive-valence scores (25 observations from 8 participants; β = 17.69; 95% CI 3.68–31.71; P = 0.0156). h, Strategies associated with an increase in the NF signal had lower arousal scores (28 observations from 9 participants; β = −18.52, 95% CI −33.22 to −3.81, P = 0.0156). These three strategy effects were nominally significant but did not remain significant after FDR correction across the ten cognitive dimensions (q = 0.052 for each).

Supplementary Files

This is a list of supplementary files associated with this preprint. Click to download.

- Supplementarymaterials.pdf